JOURNAL OF MATERIALS SCIENCE 21 (1986) 793–798

Crystallization of amorphous Zr–Ni alloys in the presence of H_2, CO, O_2, N_2 and argon gases

K. AOKI, T. MASUMOTO
The Research Institute for Iron, Steel and Other Metals, Tohoku University, Sendai 980, Japan
C. SURYANARAYANA
Centre of Advanced Study, Department of Metallurgical Engineering, Banaras Hindu University, Varanasi 221 005, India

The gas absorption and crystallization behaviour of melt-quenched amorphous $Zr_{37}Ni_{63}$ and $Zr_{67}Ni_{33}$ alloys in H_2, CO, O_2, N_2 and argon atmospheres were investigated. Unexpectedly, the nickel-rich amorphous alloy was more reactive than the zirconium-rich one. Thus, a-$Zr_{37}Ni_{63}$ can absorb hydrogen, form the metastable tetragonal ZrO_2 by oxidation and decompose into the non-equilibrium nickel, ZrC, ZrO_2(T) and ZrO_2(M) phases in CO atmosphere below its crystallization temperature. However, neither absorption of N_2 nor formation of ZrN was detected. On the contrary, the a-$Zr_{67}N_{33}$ alloy hardly reacts with gases below its crystallization temperature. The role of the surface oxide layer in gas absorption is discussed.

1. Introduction

The realization that amorphous alloys prepared by melt quenching have outstanding mechanical, electrical and magnetic properties has accelerated the pace of research in this exciting area [1, 2]. Recently, considerable attention has been paid to studying the hydrogen absorption and catalytic characteristics of amorphous alloys. For instance, it has been reported that zirconium-based Zr–Ni and Zr–Pd amorphous alloys absorb considerable quantity of hydrogen [3–6] and act as catalysts for the hydrogenation of carbon monoxide [7]. Since hydrogen absorbers or catalysts are generally used in the presence of reactive gases at elevated temperatures, it becomes imperative to evaluate the thermal stability and crystallization behaviour of amorphous alloys under these conditions. Although crystallization studies on amorphous alloys have so far been conducted mainly in a vacuum or in the presence of an inert gas [8], there is practically no report of a study in the presence of reactive gases. Furthermore, it is also of interest to know if amorphous Zr–Ni alloys can absorb gases other than hydrogen, namely oxygen, nitrogen or carbon monoxide, because of the great affinity of zirconium for these gases.

The results of a detailed investigation on the interaction during continuous heating of amorphous Zr–Ni alloys with some gases form the subject matter of the present paper.

2. Experimental procedures

$Zr_{37}Ni_{63}$ and $Zr_{67}Ni_{33}$ master alloys were prepared from high-purity metals (99.6% zirconium and 99.9% nickel) by arc melting under a protective argon atmosphere. Amorphous ribbons of about 1 mm width and 50 μm thickness were produced from these alloys under an argon atmosphere by the melt-spinning method. X-ray diffraction experiments using Cu$K\alpha$ radiation from an X-ray monochromator confirmed that the samples were amorphous. In order to evaluate the gas absorption and crystallization behaviour of the amorphous samples, differential thermal analysis (DTA) and thermogravimetric analysis (TG) were done simultaneously using the Sinku-Riko (Yokohama, Japan) high-pressure DTA–TG (Model HP–TGD–3000) at a heating rate of 10 K min^{-1} in H_2, CO, N_2, and argon gases and air at 0.1 MPa pressure. The weight of the sample used was 500 mg and the sensitivity of TG was $\pm 0.1\%$. The nature of the observed heat effect was determined by heating the samples to distinct stages in the DTA run, followed by a rapid cooling to room temperature and subjecting them to X-ray diffraction (XRD).

3. Results

3.1. a-$Zr_{37}Ni_{63}$

Fig. 1 shows the DTA and TG curves of the nickel-rich amorphous (a-) $Zr_{37}Ni_{63}$ alloys heated in different atmospheres. XRD patterns taken from samples heated to distinct stages are shown in Figs. 2 to 4. As seen in Figs. 2d and e, the XRD patterns of the sample heated to 820 and 880 K in an inert argon atmosphere clearly reveal that Zr_7Ni_{10} and Zr_2Ni_5 phases are formed when annealed at temperatures corresponding to the first and second exothermic peak, respectively, in agreement with previous reports [9, 10]. Thus, it can be concluded that the exothermic peaks above about 800 K are due to crystallization of the amorphous alloy. DTA and TG curves as well as the XRD pattern (not shown) of the sample heated in N_2 gas are very similar to those of the sample exposed to argon, and neither absorption of N_2 nor formation of ZrN is observed. On the other hand, an additional broad exothermic peak accompanying the weight increment is seen in the DTA curves of the samples examined in H_2, air and CO atmosphere.

0022–2461/86 $03.00 + .12

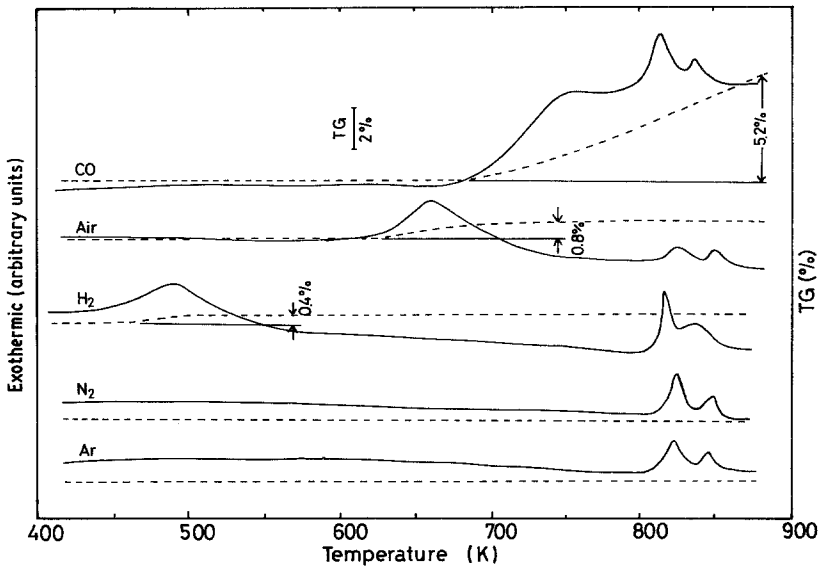

Figure 1 (———) Differential thermal analysis (DTA) and (– – –) thermogravimetric analysis (TG) curves of amorphous $Zr_{37}Ni_{63}$ heated in the presence of different gases at 0.1 MPa.

Fig. 2b shows the basic profile of the XRD pattern of the sample heated to 650 K in H_2 atmosphere. It can be observed that this pattern is similar to the as-quenched one and characterized by a broad peak typically observed in many amorphous alloys. However, one can see that there is a peak shift towards the lower-angle side, indicating that hydrogen has caused volume expansion of the sample. Thus, the broad exothermic peak around 500 K in Fig. 1 is not due to crystallization, but is due to hydrogen absorption. The XRD pattern of the sample heated to 890 K shows diffraction peaks corresponding to zirconium hydride ZrH_2 (Fig. 2c), in addition to those of the compound Zr_2Ni_5. It should be noted here, however, that the diffraction peaks corresponding to the compound Zr_7Ni_{10}, which is also a constituent of the alloy, are absent.

The XRD patterns of the samples heated to 650 and 753 K in air (Figs. 3a and b) show crystalline peaks superimposed on an amorphous background. The peaks in the sample heated to 650 K can be indexed on the basis of the tetragonal $ZrO_2(T)$ structure, enabling us to conclude that the exothermic peak around 650 K

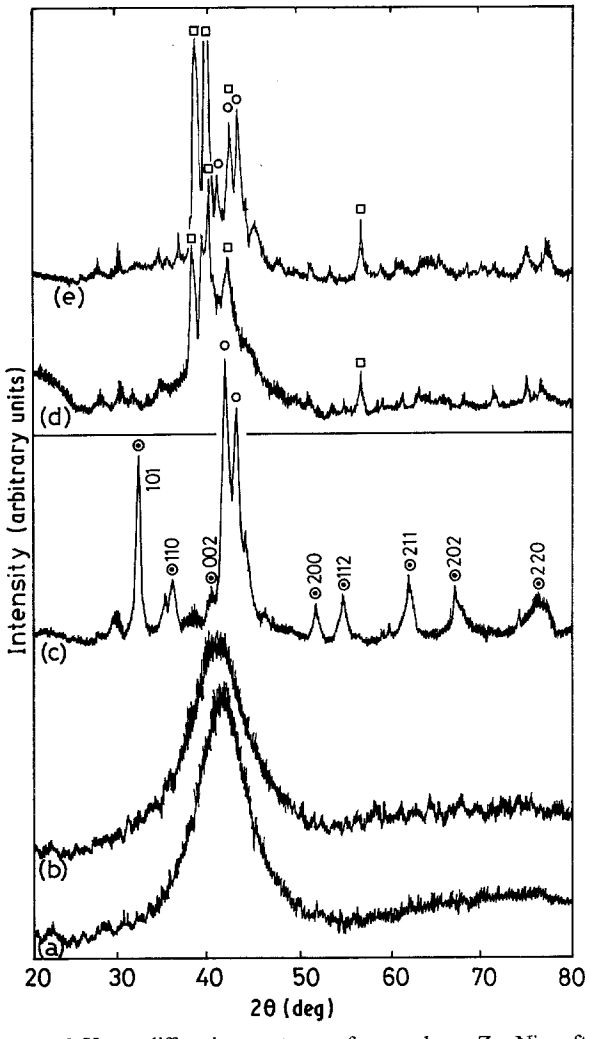

Figure 2 X-ray diffraction patterns of amorphous $Zr_{37}Ni_{63}$ after heating to 0.1 MPa gas pressure to distinct stages of DTA. Run in H_2 (a) as-quenched, (b) heated to 650 K and (c) heated to 890 K; and in argon (d) heated to 820 K and (e) heated to 890 K. Peaks are (○) Zr_2Ni_5, (⊙) ZrH_2, (□) Zr_7Ni_{10}.

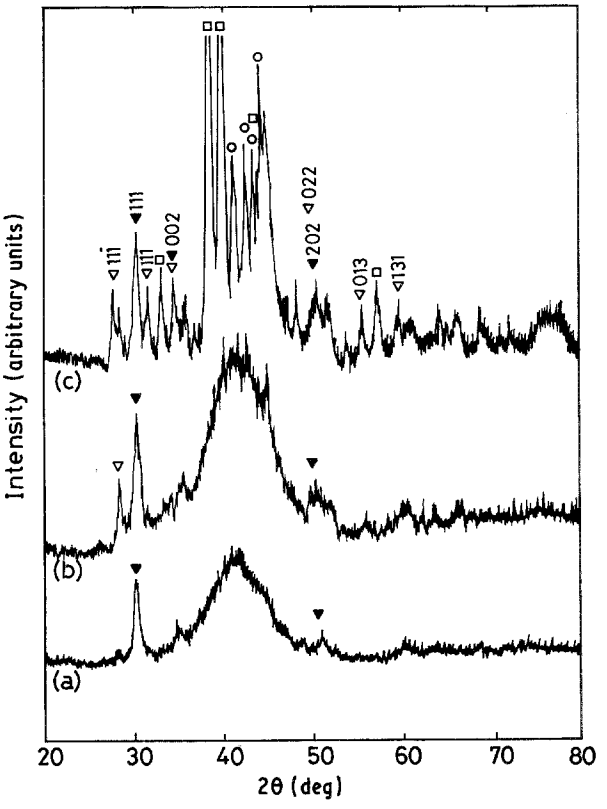

Figure 3 X-ray diffraction patterns of a-$Zr_{37}Ni_{63}$ heated to distinct stages in air at 0.1 MPa: (a) 650 K, (b) 753 K, (c) 880 K. (▼) $ZrO_2(T)$, (▽) $ZrO_2(M)$, (○) Zr_2Ni_5, (□) Zr_7Ni_{10}.

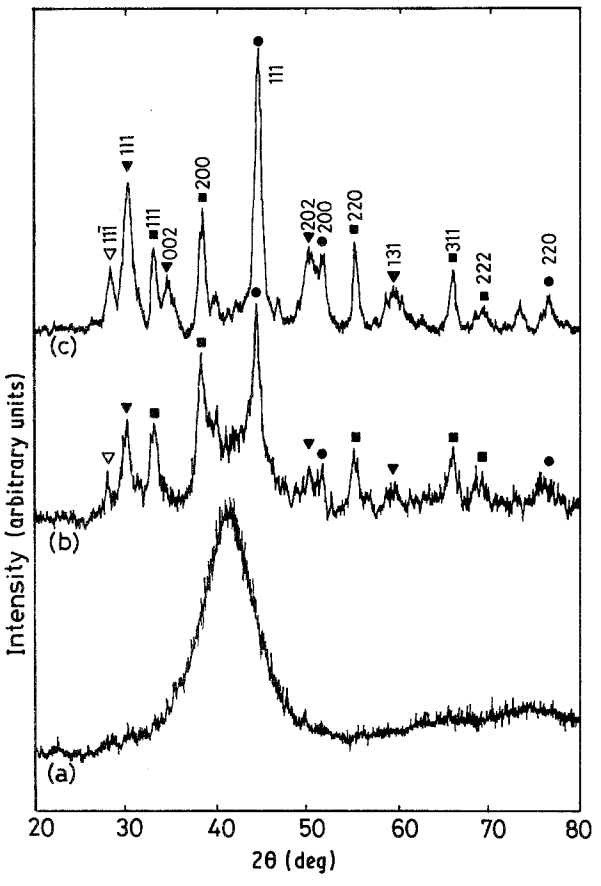

Figure 4 X-ray diffraction patterns of a-$Zr_{37}Ni_{63}$ (a) as-quenched and heated to (a) 773 and (b) 873 K in CO atmosphere at 0.1 MPa. (▼) ZrO_2(T), (▽) ZrO_2(M), (●) Ni, (■) ZrC.

in Fig. 1 is due to oxidation of the sample. At the higher temperature of 753 K, monoclinic ZrO_2(M) is also formed. The XRD pattern of the sample heated to 880 K shows two crystalline peaks of Zr_2Ni_5 and Zr_7Ni_{10} in addition to those of the oxides.

In CO atmosphere, a prominent weight increment is observed above about 700 K as seen in Fig. 1. The XRD pattern of the sample heated to 773 K shows the differential peaks of nickel, ZrC, ZrO_2(T) and ZrO_2(M) superimposed on an amorphous broad halo, but both Zr_2Ni_5 and Zr_7Ni_{10} are totally absent. Fig. 5 shows the electron probe microanalysis (EPMA) results of line analysis of the transverse cross-section of an amorphous sample heated to 773 K in CO atmosphere.

It can be seen that reaction products about 1 μm in thickness are formed on both sides of the sample. An inner non-reacted region is retained in the amorphous state, which crystallizes at higher temperatures as shown by the exothermic peaks in Fig. 1.

Figs. 6a and b show scanning electron micrographs of the samples heated to 900 K in H_2 and CO gas, respectively. The surface of the former is flat and featureless as reported previously [11], while many particles seem to be attached to the surface of the latter. The XRD pattern of these powder particles is shown in Fig. 7, which indicates the presence of nickel, ZrO_2(T) and ZrO_2(M). However, in contrast to the pattern shown in Fig. 4c, the ZrC phase is not present in the powdery particles, implying that ZrC is strongly bonded to the sample.

Table I presents the reaction temperatures T_r, crystallization temperatures T_x, weight changes and phases present after crystallization for a-$Zr_{37}Ni_{63}$ alloys. In the present work, T_r and T_x were defined as the temperatures corresponding to the intersection of the extrapolated base line and the steepest tangent to the exothermic peak.

3.2. a-$Zr_{67}Ni_{33}$

DTA and TG curves of the zirconium-rich amorphous $Zr_{67}Ni_{33}$ alloys are shown in Fig. 8. XRD patterns of the as-prepared and crystallized samples are collectively shown in Fig. 9. From these figures, it appears that no gas absorption takes place in these samples in the amorphous state in contrast to the nickel-rich a-$Zr_{37}Ni_{63}$. In all atmospheres except hydrogen, the a-$Zr_{67}Ni_{33}$ alloy crystallizes directly into the compound Zr_2Ni as indicated by the single exothermic peak, in conformity with previous reports [10, 12]. In H_2 gas, however, the alloy appears to crystallize into the Zr_7Ni_{10} phase along with the formation of the hydride ZrH_2. Furthermore, in air slight oxidation of the sample takes place after crystallization. The major oxide in this case is monoclinic ZrO_2. Weight changes, crystallization temperatures and the phases present following crystallization are presented in Table II for a-$Zr_{67}Ni_{33}$.

4. Discussion

From both thermal analysis and XRD patterns, it was

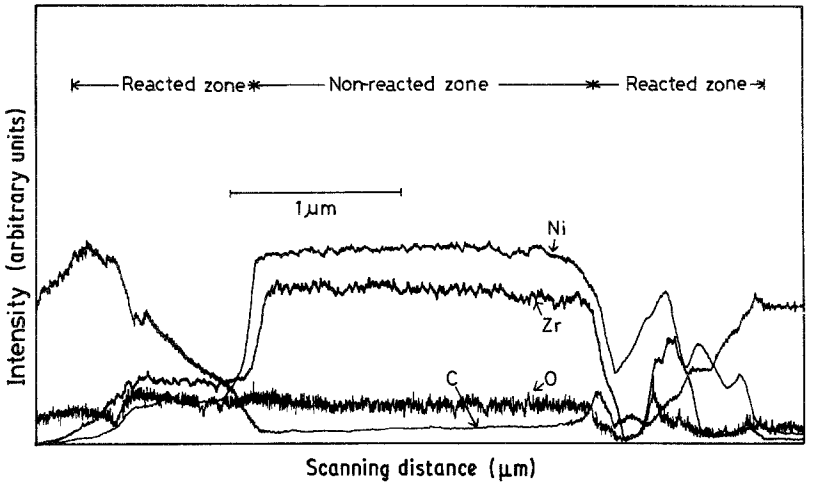

Figure 5 EPMA line analysis of a transverse section of amophous $Zr_{37}Ni_{63}$ heated to 773 K in CO gas.

TABLE I Properties of amorphous $Zr_{37}Ni_{63}$ alloys after exposure to different atmospheres

Atmosphere	Reaction temperature T_r(K)	Reaction	Crystallization temperature T_x(K)	Weight increment (%)	Phases present after crystallization
CO	684	Oxidation–carbonization	802	5.2	Ni, ZrC, ZrO_2(T), ZrO_2(M)
Air	626	Oxidation	814	0.8	ZrO_2(T), ZrO_2(M), Zr_7Ni_{10}, Zr_2Ni_5
H_2	466	Hydrogen absorption	812	0.4	ZrH_2, Zr_2Ni_5
N_2	–	–	814	–	Zr_7Ni_{10}, Zr_2Ni_5
Argon	–	–	812	–	Zr_7Ni_{10}, Zr_2Ni_5

clearly shown that zirconium-rich a-$Zr_{67}Ni_{33}$ hardly reacts with different gases below its crystallization temperature, while nickel-rich a-$Zr_{37}Ni_{63}$ absorbs hydrogen and also gets oxidized in the same temperature range. Further, a-$Zr_{37}Ni_{63}$ decompose into nickel, ZrC, ZrO_2(T) and ZrO_2(M) in CO atmosphere at higher temperatures. Thus, the nickel-rich amorphous alloy appears to be more reactive than the zirconium-rich alloy, which appears to be contradictory to the accepted fact that the latter should be more reactive. This is indicated by the fact that the free energy of formation of ZrH_2, ZrO_2, ZrN and ZrC are considerably lower than that for nickel-rich compounds. We shall now discuss the reasons for this unexpected behaviour.

Interaction between amorphous alloys and gases leading to absorption, hydriding, oxidation, etc. depends to a large extent on the surface condition of the as-quenched sample and also on the nature of the phases, thickness and mechanical properties of the surface oxide layers. In the present case, the oxide layers on the as-quenched Zr–Ni alloys were too thin to enable their structures to be identified by X-ray diffraction. However, tetragonal ZrO_2 could be identified on the nickel-rich a-$Zr_{37}Ni_{63}$ alloy after heating in air, while no oxide could be identified in the zirconium-rich a-$Zr_{67}Ni_{33}$ alloy heated to the same temperature. Thus, it appears that thick and strongly adherent oxide layers are formed on the zirconium-rich alloy during the melt quenching operation, and these prevent low-temperature oxidation.

In addition to the thickness, one should also consider the structure of the oxide layer. As is well known, there are three well-defined polymorphs of pure ZrO_2 with monoclinic, tetragonal and cubic structures [13]. The monoclinic phase is stable up to about 1400 K, at about which temperature it transforms to the tetragonal phase. Since tetragonal ZrO_2 cannot be retained on quenching [13], ZrO_2(T) present in the a-$Zr_{37}Ni_{63}$ alloy can be considered a metastable phase. It has been shown earlier that metastable ZrO_2(T) can exist even at very low temperatures when the crystal size is smaller than 30 nm or when the oxide is stabilized with the help of another element [14]. The presence of nickel in a-$Zr_{37}Ni_{63}$ alloy may have been responsible for the stabilization of ZrO_2(T) in this case. According to Spit *et al.* [14], monoclinic ZrO_2 inhibits the absorption of hydrogen, while the metastable tetragonal ZrO_2 is porous and hydrogen can penetrate through it.

Based on the propositions of Spit *et al.* [14], the difference in hydrogen absorption behaviour between a-$Zr_{37}Ni_{63}$ and a-$Zr_{67}Ni_{33}$ can be explained as follows. Amorphous $Zr_{67}Ni_{33}$ is covered with such a thick layer of monoclinic ZrO_2 that this alloy may not absorb any hydrogen. On the other hand, a-$Zr_{37}Ni_{63}$ can absorb hydrogen easily, because it is covered with the tetragonal ZrO_2. However, if the a-$Zr_{67}Ni_{33}$ alloy is held for a long period below its crystallization temperature in high-pressure hydrogen, it can absorb large quantity of hydrogen as reported earlier [10, 11].

Crystallization of a-$Zr_{67}Ni_{33}$ results in a considerable volume change leading to the formation of cracks in the surface oxide layers. Hydrogen can penetrate into the interior of the sample through these cracks and as

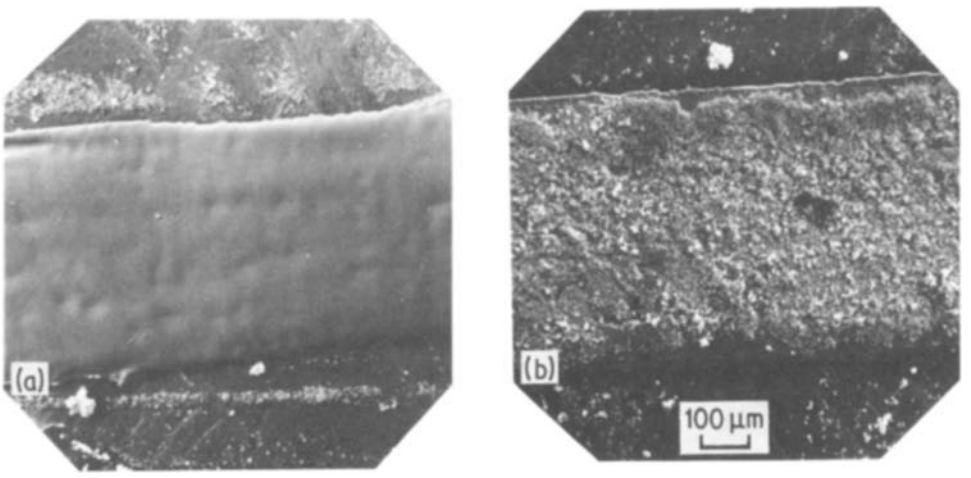

Figure 6 Scanning electron micrographs of amorphous $Zr_{37}Ni_{63}$ heated to 900 K in (a) H_2 and (b) CO gas.

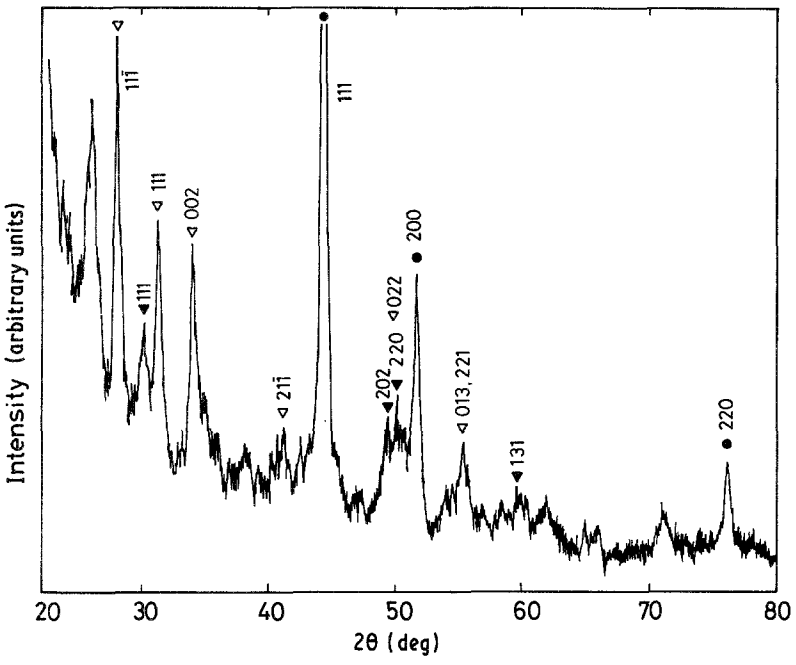

Figure 7 X-ray diffraction pattern of the powder particles formed on the surface of a-Zr_3Ni_{63} heated to 900 K in CO gas at 0.1 MPa. (▼) ZrO_2(T), (▽) ZrO_2(M), (●) Ni.

a result zirconium hydride, ZrH_2, forms at the crystallization point as seen in Fig. 5.

Next, we consider the formation of the non-equilibrium phases nickel, ZrC, ZrO_2(T) and ZrO_2(M) in CO atmosphere. It is well known that nickel is a catalyst for the dissociation of CO gas. When the nickel-rich a-$Zr_{37}Ni_{63}$ is heated in CO atmosphere, some CO molecules may dissociate into carbon and oxygen atoms through the catalysis by nickel. Since zirconium has a very strong affinity towards carbon and oxygen as can be seen from free-energy data for the formation of ZrC and ZrO_2, both ZrC and ZrO_2 are easily formed near the surface region.

Formation of these compounds leads to a relative increase in the nickel concentration, which continues till the appearance of pure nickel. Thus, as a result of the carbonization and oxidation of zirconium, pure nickel appears. The formation of nickel, ZrC and ZrO_2 clearly suggest that a-$Zr_{37}Ni_{63}$ alloy can act as a catalyst for the dissociation of CO gas in contrast to a-$Zr_{67}Ni_{33}$. Thus, it is expected to be a potential candidate as a catalyst for the hydrogenation of CO as reported previously [7].

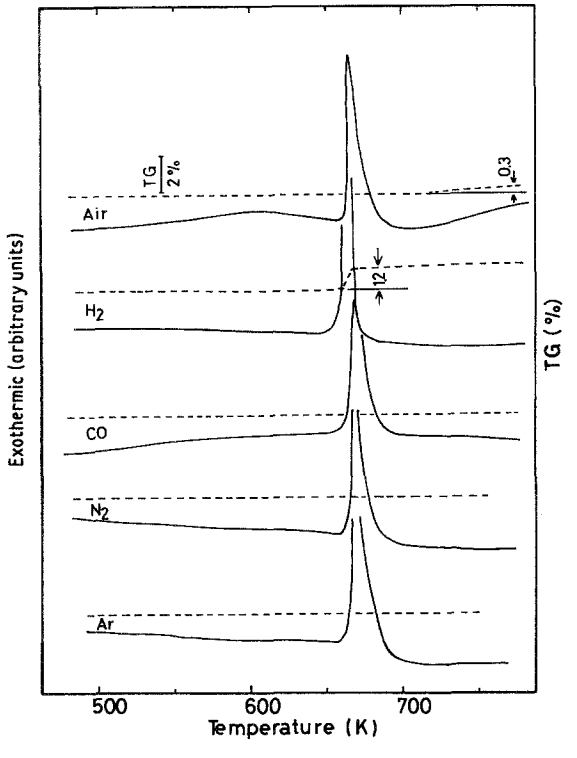

Figure 8 (———) DTA and (– – –) TG curves of amorphous $Zr_{67}Ni_{33}$ heated in different gaseous atmospheres at 0.1 MPa.

5. Conclusions

The gas absorption and crystallization characteristics of amorphous Zr–Ni alloys, prepared by melt

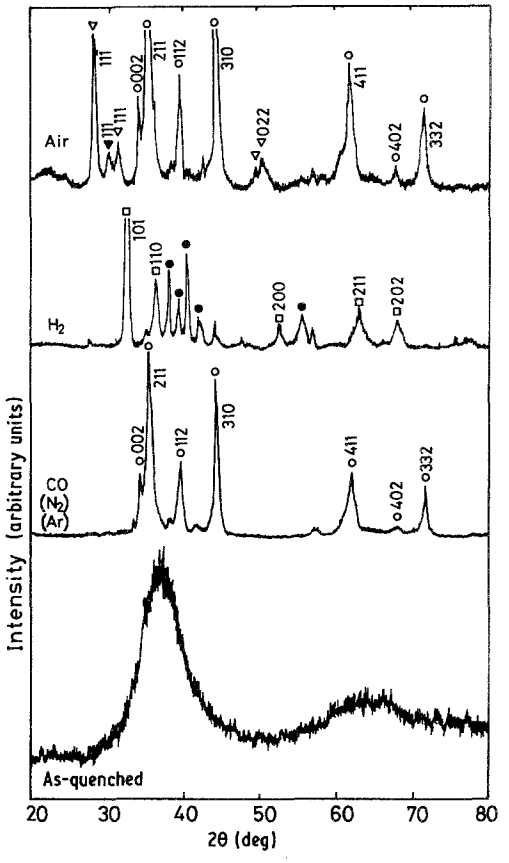

Figure 9 X-ray diffraction patterns of a-$Zr_{67}Ni_{33}$ heated to 800 K in the presence of different gases. (○) Zr_2Ni, (▼) ZrO_2(T), (▽) ZrO_2(M), (□) ZrH_2, (●) Zr_7Ni_{10}.

TABLE II Properties of a-$Zr_{67}Ni_{33}$ after exposure to different atmospheres

Atmosphere	Crystallization temperature T_x(K)	Weight increment (%)	Phases present after crystallization
Air	664	0.3	Zr_2Ni, ZrO_2(M)
H_2	658	1.2	ZrH_2, Zr_7Ni_{10}
CO	663	–	Zr_2Ni
N_2	664	–	Zr_2Ni
Argon	664	–	Zr_2Ni

quenching, were investigated by differential thermal analysis, thermogravimetric analysis and X-ray diffraction techniques in the presence of H_2, CO, N_2, argon and air. The main conclusions of the present study are as follows. The nickel-rich amorphous $Zr_{37}Ni_{63}$ alloy absorbs hydrogen, forms metastable tetragonal ZrO_2 by oxidation and decomposes to form non-equilibrium nickel, ZrC, ZrO_2(T), ZrO_2(M) phases in CO atmosphere below its crystallization temperature. However, neither absorption of N_2 nor formation of ZrN was detected in a-$Zr_{37}Ni_{63}$. On the contrary, the zirconium-rich amorphous $Zr_{67}Ni_{33}$ hardly reacts with gases below its crystallization temperature, because the monoclinic oxide layers prevent direct contact between the gases and the alloy. Since the nickel-rich amorphous Zr–Ni alloy can absorb hydrogen and can dissociate CO gas, it is expected to be a candidate catalyst for hydrogenation of CO.

References

1. C. SURYANARAYANA, "Rapidly Quenched Metal – a Bibliography 1973–1979" (IFI Plenum, New York, 1980), p. 2.
3. F. H. M. SPIT, J. W. DRIJVER and S. RADELAAR, *Scripta Metall.* **14** (1980) 1071.
4. K. AOKI, A. HORATA and T. MASUMOTO, in Proceedings of the 4th International Conference on Rapidly Quenched Metals, Vol. 2, edited by T. Masumoto and K. Suzuki (Japan Insitute of Metals, Sendai, 1982) p. 1649.
5. K. AOKI, M. KAMACHI and T. MASUMOTO, *J. Non-Cryst. Solids* **61/62** (1984) 679.
6. K. KAI, T. FUKUNAGA, T. NOMOTO, N. WATANABE and K. SUZUKI, in Proceedings of the 4th International Conference on Rapidly Quenched Metals, Vol. 2, edited by T. Masumoto and K. Suzuki (Japan Institute of Metals, Sendai, 1982) p. 1609.
7. A. YOKOYAMA, H. KOMIYAMA, H. INOUE, T. MASUMOTO and H. M. KIMURA, *Chem. Lett.* (1983) 195.
8. S. RANGANATHAN and C. SURYANARAYANA, in Proceedings of Seminar on Phase Stability and Phase Transformations, *Mater. Sci. Forum* **3** (1985) 173.
9. Y. D. DONG, G. GREGAN and M. G. SCOTT, *J. Non-Cryst. Solids* **43** (1981) 403.
10. K. AOKI and T. MASUMOTO, *J. Jpn. Inst. Metals* **49** (1985) 89.
11. K. AOKI, M. KAMACHI and T. MASUMOTO, *Sci. Rep. Res. Inst. Tohoku Univ.* **A-31** (1983) 191.
12. M. G. SCOTT, G. GREGAN and Y. D. DONG, in Proceedings of the 4th International Conference on Rapidly Quenched Metals, Vol. 1, edited by T. Masumoto and K. Suzuki (Japan Institute of Metals, Sendai, 1982) p. 671.
13. R. C. GARVIE, in "High Temperature Oxide II," edited by A. M. Alper (Academic Press, New York, 1972) p. 117.
14. F. H. M. SPIT, K. BLOC, E. HENDRIC, G. WINKELS, W. TURKENBURG, J. DRIJVER and S. RADELAAR, in Proceedings of the 4th International Conference on Rapidly Quenched Metals, Vol. 2, edited by T. Masumoto and K. Suzuki (Japan Institute of metals, Sendai, 1982) p. 1635.

Received 22 March
and accepted 16 April 1985